Alkyl Sulfonyl Fluorides as Ambiphiles in the Stereoselective, Palladium(II)-Catalyzed Cyclopropanation of Unactivated Alkenes

Yilin Cao[a], Warabhorn Rodphon[a], Turki M. Alturaifi[b], Al Vicente Riano D. Lisboa[a], Zhouyang Ren[a], Job J. C. Struijs[a], Hui-Qi Ni[a], Taras Savchuk[c,d], Pavel K. Mykhailiuk[c,e], Richard P. Loach[f], Shouliang Yang[g], Indrawan J. McAlpine[g,f], Donna G. Blackmond[a], Peng Liu[b*], K. Barry Sharpless[a*], and Keary M. Engle[a*]

[a] Department of Chemistry, The Scripps Research Institute, 10550 North Torrey Pines Road, La Jolla, California 92037, United States

[b] Department of Chemistry, University of Pittsburgh, 219 Parkman Avenue, Pittsburgh, Pennsylvania 15260, United States

[c] Enamine Ltd., Chervonotkatska 78, 02094 Kyiv, Ukraine

[d] Taras Shevchenko National University of Kyiv, Faculty of Chemistry, Volodymyrska 60, 01601 Kyiv, Ukraine

[e] Kukhar Institute of Bioorganic Chemistry and Petrochemistry NAS of Ukraine, 02094 Kyiv, Ukraine

[f] Pfizer Medicinal Sciences, Eastern Point Road, Groton, Connecticut 06340, United States

[g] Pfizer Oncology Medicinal Chemistry, 10770 Science Center Drive, San Diego, California 92121, United States

[h] Genesis Therapeutics, 11568 Sorrento Valley Rd. Suite 8, San Diego, California 92121, United States

ABSTRACT: The ambiphilic reactivity of alkyl sulfonyl fluorides in the stereoselective synthesis of diverse cyclopropanes from olefins under palladium(II) catalysis is presented. The sulfonyl fluoride functionality serves as both an acidifying group and an internal oxidant within the ambiphile, enabling the successive carbopalladation and oxidative addition steps in the catalytic cycle, respectively. The transformation grants access to *cis*-substituted cyclopropanes and exhibits broad compatibility with various alkyl sulfonyl fluorides, including those bearing –CN, $-CO_2R$, isoxazolyl, pyrazolyl, and aryl groups. With internal alkene substrates, 1,2,3-trisubstituted cyclopropanes that are otherwise challenging to synthesize are formed in good to moderate yield and predictable diastereoselectivity. Detailed mechanistic insights from reaction progress kinetic analysis (RPKA) and density functional theory (DFT) calculations reveal that the S_N2-type C–SO_2F oxidative addition is the turnover-limiting and diastereoselectivity-determining step.

Organosulfonyl fluorides have emerged as central players in organic synthesis,[1,2] owing to the rise of sulfur(VI) fluoride exchange ($SuFE_X$) chemistry, which allows for rapid and reliable diversification through nucleophilic displacement of fluoride with oxygen and nitrogen nucleophiles.[3-5] The utility of organosulfonyl fluorides in this context has motivated the development of a growing number of methods to synthesize structurally diverse sulfonyl fluorides in an efficient, selective, and modular manner (Scheme 1A).[6]

In contrast to widely studied aryl-[7-9], alkenyl-[10-12], and alkynyl sulfonyl fluorides[6e], alkyl sulfonyl fluorides have been less thoroughly investigated despite offering unique opportunities as synthetic building blocks owing to the acidifying effect of the sulfonyl group on the α-protons.[4] Prior work has demonstrated the utility of alkyl sulfonyl fluorides in C–C bond formation through reaction with classical electrophiles, such as alkyl halides and carbonyl compounds, in the presence of base (Scheme 1B).[13-16] We surmised that alkyl sulfonyl fluorides could exhibit unique ambiphilic reactivity in transition metal catalysis, capitalizing on the ability of the sulfonyl fluoride group to serve the dual role as a pronucleophile activator and electrophilic reactive group (i.e. internal oxidant).

Our lab previously developed a palladium-catalyzed *anti*-cyclopropanation of olefins with various carbon pronucleophiles and I_2 as the bystanding oxidant, where the hypothesized mechanism involves initial α-iodination of the nucleophile, directed carbopalladation, Pd^{II}/Pd^{IV} oxidative addition of the newly formed C(sp^3)–I bond, and finally C(sp^3)–C(sp^3) reductive elimination from the palladacyclobutane intermediate.[17] The need for doubly activated carbon pronucleophiles in all cases but nitromethane limits the scope of substituted cyclopropanes that can be accessed with this method, leading us to search for alternative nucleophilic coupling partners in which a leaving group and an acidifying group could be merged into the same entity.

Herein, we demonstrate alkyl sulfonyl fluorides acting as ambiphilic coupling partners in the stereoselective cyclopropanation of unactivated olefins through the Pd^{II}/Pd^{IV} redox couple,[18] delivering stereochemical outcomes that are inaccessible using conventional leaving groups (Scheme 1B).

Scheme 1. Background and This Work

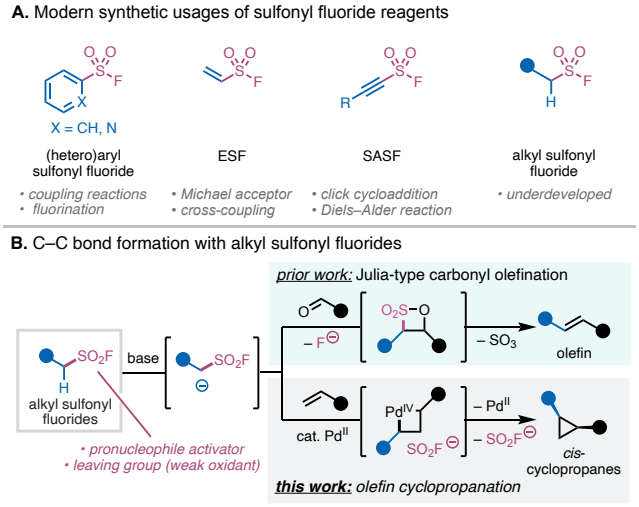

In this context, alkenyl amide **1a** and alkyl sulfonyl fluoride **2a** were selected as model substrates. After extensive screening, we identified optimal reaction conditions using a combination of $Pd(OAc)_2$ (10 mol%) and Na_2CO_3 (1.0 equiv) in DMA (0.33 M) under a nitrogen atmosphere to afford cyclopropane **3aa** in 99% yield with 98:2 *d.r.*; the unusual *cis*-configuration of the major product was confirmed by single-crystal X-ray diffraction.[19] Key findings from our optimization campaign include the important role of Na_2CO_3 as the base, as other carbonate salts, such as K_2CO_3 and Cs_2CO_3, led to substantially lower yields (entries 2–3), as did bases with other counteranions (entries 4–5). Other commonly used Pd^{II} sources, such as $PdCl_2$ and $Pd(TFA)_2$, gave slightly lower yields and comparable diastereoselectivity (entries 6–7). Increasing the concentration of the reaction mixture decreased the yield (entry 8). The use of a polar aprotic solvent was crucial, and DMF and DMSO were reasonably effective alternatives to DMA (entries 9–11). We were also pleased to find that the reaction gave 92% yield even when set up and run under air (entry 12). In control experiments, we found that changing the leaving group to sulfonyl chloride (**LG2**), phenyl sulfonyl (**LG3**), or methyl sulfonyl (**LG4**) groups led to no reaction or trace product formation (entry 13–14), indicating that the sulfonyl fluoride is key for the observed reaction. A representative sulfonium bromide sulfur ylide precursor (**LG5**) gave moderate yields but poor *d.r.* (entry 15). Beyond sulfur-based leaving groups, halides were also tested but found to be ineffective (entry 16).

Table 1. Optimization of palladium(II)-catalyzed cyclopropanation of unactivated alkenes

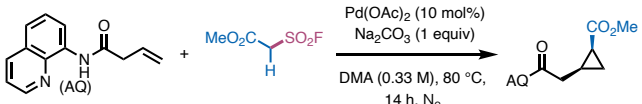

1a, 1 equiv + **2a**, 3 equiv → **3aa** [X-ray]

entry	deviation from standard conditions	yield of **3aa** (%)[a]	*d.r.*[c]
1	none	99 (94)[b]	98:2
2	K_2CO_3	34	94:6
3	Cs_2CO_3	3	-
4	NaF	74	96:4
5	KF	60	97:4
6	$PdCl_2$	95	95:5
7	$Pd(TFA)_2$	95	98:2
8	1.0 M DMA	75	96:4
9	DMF	76	95:5
10	DMSO	36	97:3
11	1,2-DCE, toluene, THF	n.d.	-
12	DMA, air	92	96:4
13	**LG2** instead of **LG1**	9	60:40
14	**LG3, LG4** instead of **LG1**	n.d.	-
15	**LG5** instead of **LG1**	72	64:36
16	**LG6, LG7, LG8** instead of **LG1**	trace	-

-SO_2F	-SO_2Cl	-SO_2Ph	-SO_2Me
LG1	**LG2**	**LG3**	**LG4**
99%, 98:2 *d.r.*	9%, 60:40 *d.r.*	n.d.	n.d.
-$SMe_2^{\oplus}$	-I	-Br	-Cl
LG5	**LG6**	**LG7**	**LG8**
72%, 64:36 *d.r.*	trace	trace	trace

[a]Reactions performed on 0.1 mmol scale. Yields were determined by ^1H NMR analysis of the crude reaction mixture with benzyl 4-fluorobenzoate as an internal standard. n.d. = not detected. [b]Isolated yield shown in parentheses. [c]Diastereomeric ratio (*d.r.*) was determined by ^1H NMR analysis of the crude reaction mixture.

In seeking to rationalize the optimization data, we considered previous reports that found alkyl sulfonyl fluorides, such as phenyl methyl sulfonyl fluoride (PMSF), to be highly unstable in aqueous solutions.[20] We questioned whether yield differences could be partially attributed to the competitive decomposition of the nucleophile under different conditions (i.e., in different solvents and in the presence or absence of adventitious water). To this end, we examined the stability of alkyl sulfonyl fluoride **2a** in DMA, DMF, and DMSO (Table 2 and Supporting Information for details). Surprisingly, alkyl sulfonyl fluoride **2a** was fully decomposed in anhydrous DMSO after 2 hours but proved to be relatively stable in anhydrous DMF. Similarly, we found no decomposition of alkyl sulfonyl fluoride **2a** in anhydrous DMA under an inert atmosphere. However, under air moderate levels of decomposition in DMA could be detected, and complete decomposition was observed in wet DMA. These results indicate that the rate of decomposition of **2a** is dependent on the solvent identity and amount of adventitious water in the solution.

Table 2. Nucleophile 2a stability test[a]

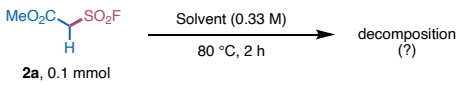

solvent	H_2O content	atmosphere	remaining **2a**
DMA	wet	air	<5%
DMA	anhydrous	air	83%
DMA	anhydrous	N_2	100%
DMF-d_7	anhydrous	N_2	85%
DMSO-d_6	anhydrous	N_2	<5%

[a]Reactions performed on 0.1 mmol scale. Percentages represent ^{1}H NMR yields using CH_2Br_2 as internal standard.

Having optimized the conditions, we began investigating the scope with respect to the alkyl sulfonyl fluoride (Table 3). The reaction proceeded in moderate to excellent yield with various ester nucleophiles, including *tert*-butyl ester (**3ac**), benzyl ester (**3ad**), allyl ester (**3ae**), and phenyl ester (**3af**). Amide or nitrile-based coupling partners (**3ag**–**3h**) led to diminished yield but maintained excellent *cis*-diastereoselectivity (>20:1). We found that the reaction could tolerate weaker electron-withdrawing groups, including a 2-bromopropenyl group (**3ai**) and various heterocycles, including isoxazole (**3aj**) and 1-methyl-1*H*-pyrazole (**3ak**), which gave 32%, 43%, and 20% yield, respectively. An α-aryl alkyl sulfonyl fluoride nucleophile participated in the reaction to form a fully substituted carbon center within the cyclopropane, albeit in moderate yield and *d.r.* (**3al**). Aryl-substituted methylene sulfonyl fluorides were also investigated. Interestingly, the reaction did not proceed with unsubstituted, electron-neutral benzylsulfonyl fluoride, but proceeded with substituted benzylsulfonyl fluoride substrates bearing electron-withdrawing groups at the *para*-position (**3am**–**3ap**). Stronger electron-withdrawing groups led to improved yields and diastereoselectivity. Additionally, a *meta*-nitro substrate was also tolerated (**3aq**).

Next, the scope of alkenes was investigated. Internal alkenes afforded good to moderate yields (**4aa**–**4ae**). Notably, (*Z*)-alkenes reacted with excellent diastereoselectivity (>20:1), affording a single diastereomer. To our delight, under the standard condition, the challenging all-*cis* cyclopropane was formed from an (*E*)-configured internal alkene in moderate yield (**4ad**). In addition, α-substituted β,γ-unsaturated amide substrates are well tolerated, giving the desired products in moderate to excellent yields (**4af**–**4ai**). Specifically, a diene substrate (**4ag**) could be chemoselectively cyclopropanated at the β,γ-alkene, while leaving the δ,ε-alkene unperturbed. When the tether length between the alkene and directing group was extended and a γ, δ-unsaturated amide was tested, the cyclopropane product was furnished in moderate yield with excellent diastereoselectivity (**4ak**).

Table 3. Substrate Scope

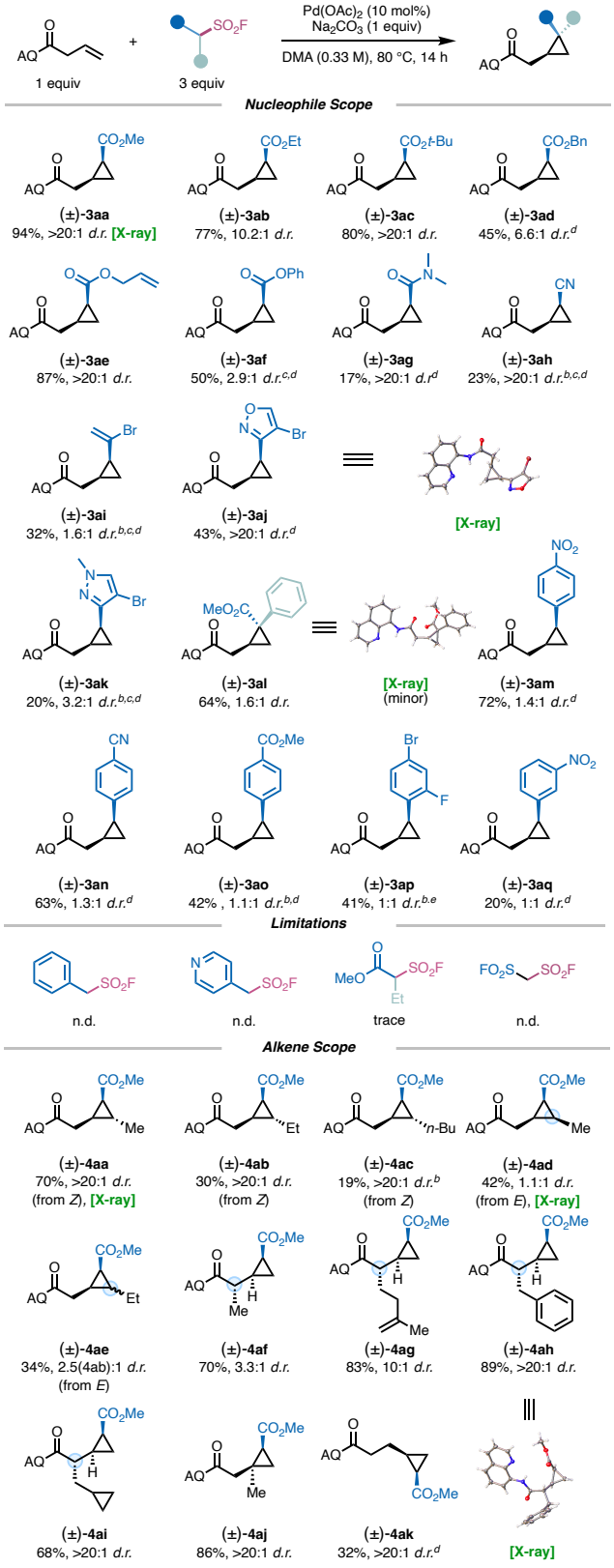

[a]Reactions performed on 0.1 mmol scale. Percentages represent isolated yields. Diastereomeric ratio (*d.r.*) was determined by ^{1}H NMR of crude or

purified reaction mixture. Diastereomeric center is highlighted with blue circle. [b]Reactions performed under 20 mol% catalyst loading. [c]Reactions performed under 5 equiv alkyl fluoride loading. [d]Reactions performed under 24 h. [e]Reactions performed under 36 h. [f]Reactions performed at 100 °C.

The methodology could be easily scaled up and performed on 1.0-mmol scale under the standard reaction conditions, giving *cis*-cyclopropane **3aa** in 86% (Scheme 2A). Performing the reaction on 100 mmol scale resulted in 81% yield with 9:1 *d.r.*. Removal of the directing auxiliary was possible through a two-step sequence.[21] Initial introduction of an *N*-Boc activating group proceeded in 83% yield (**5aa**). Then, hydrolysis with LiOOH/water gave carboxylic acid **6aa** in 86% yield on multigram-scale, which has been commercialized by Enamine (Scheme 2B). Alternatively, a representative amine could be used in the second step in a net transamidation (58% yield, **6ab**). If desired by the practitioner, the loading of nucleophile **2a** can be lowered to 1.5 equiv while maintaining comparable yield and diastereoselectivity with a dual base system (0.75 equiv NaF and 0.25 equiv Na_2CO_3) (Scheme 2C, see Supporting Information for details).

Scheme 2. Scale-Up, Directing Auxiliary Removal, and Lower Nucleophile Loading

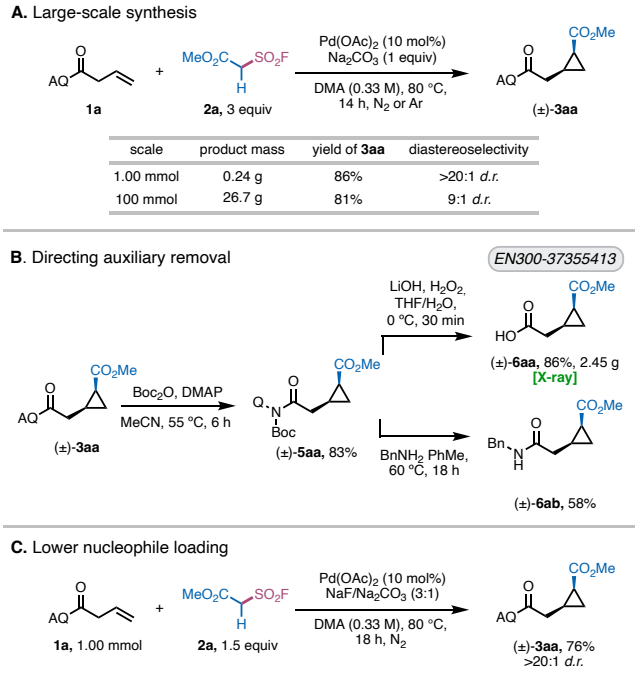

The unprecedented reactivity of alkyl sulfonyl fluorides in this cyclopropanation and the unique stereochemical outcomes prompted us to examine the mechanism through experimental and computational techniques. We performed reaction progress kinetic analysis (RPKA) to determine key mechanistic features of the reaction from a minimal number of experiments.[22] First, we compared the standard reaction profile to a "same excess" experiment that simulated 25% conversion (Scheme 3A). Time-shifting reveals that the two curves overlay for the first 50% conversion, after which a slight deviation occurs, a telltale sign of either mild product inhibition or mild catalyst deactivation. To distinguish between the two possibilities, a third experiment was performed with product **3aa** (83 mM) as an additive, and overlay with the same excess experiment confirms mild catalyst deactivation. The lack of product inhibition is notable given the capacity of the product to bind to the catalyst in a polydentate fashion. To explore potential coordination between the product and catalyst further, **3aa** was treated with $Pd(OAc)_2$ (1 equiv), resulting in the formation of *N,N,C*-palladacycle **Pd-3aa** in which the 3° C(cyclopropyl)–H bond was cleaved (Scheme 3B) as characterized by X-ray crystallography.[23] Complex **Pd-3aa** proved to be catalytically competent under the standard reaction conditions, showing the reversibility of C–H activation, consistent with the lack of product inhibition. Next, to estimate the order of the reaction components, we performed a series of "different excess" experiments (Scheme 3C). Considering that catalyst deactivation becomes more pronounced at higher conversion, we focused on the early stages of the reaction (<50% conversion). The variable time normalization analysis (VTNA)[24] plot showed both alkene [**1a**] and nucleophile [**2a**] to be close to zero-order and $Pd(OAc)_2$ to be close to first-order. Overall, the kinetic data are consistent with either oxidative addition or reductive elimination as the rate-determining step. To gain further insights into the rate-determining step, we conducted an Eyring analysis to obtain activation parameters (Scheme 3D). At temperatures close to standard conditions (70–100 °C), the experimental $\Delta S^{\ddagger}$ was determined to be -24.6 e.u. and $\Delta H^{\ddagger}$ to be 16 kcal/mol ($\Delta G^{\ddagger}_{80°C}$ = 24.7 kcal/mol). Given that large negative $\Delta S^{\ddagger}$ values are commonly observed with bimolecular associative reactions[25] and oxidative addition and reductive elimination are unimolecular steps, the data suggests potential desolvation and coordination of a ligand to the metal center in traversing from the catalyst resting state to the rate-limiting transition state along the potential energy surface, which informed subsequent density functional theory (DFT) calculations.

DFT calculations with alkene **1a** and alkyl sulfonyl fluoride nucleophile **2a** as model substrates were performed to gain insights into various facets of the catalytic cycle, including the rate- and diastereoselectivity-determining steps (Scheme 4A).[26] A particular focus was placed on the oxidative addition mechanisms and the origin of diastereoselectivity favoring the *cis*-cyclopropane product **3aa**. Ligand exchange of the precatalyst $Pd(OAc)_2$ with **1a** forms π-alkene Pd^{II} complex **Pd-1** with the 8-aminoquinoline (AQ) directing group binding to the Pd in a bidentate fashion. Two competing *anti*-nucleopalladation transition states with the deprotonated nucleophile[27-29] **2a'** were considered (**TS1** and **TS1'**), which lead to two different diastereomers of the palladacycle intermediate (**A** and **A'**, respectively). In the more stable transition state **TS1**, the largest substituent on the nucleophile, SO_2F, is placed *anti*-periplanar with the alkene C=C bond to minimize steric strain, whereas in the less stable diastereomeric transition state **TS1'**, the ester group is *anti*-periplanar with the C=C bond (Figure S4). This steric effect makes **TS1'** 3.4 kcal/mol less stable than **TS1**. Although the formation of palladacycle **A** is kinetically favored in the *anti*-nucleopalladation, diastereomers **A** and **A'** rapidly epimerize via deprotonation of the acidic α-C–H. The Na_2CO_3-mediated deprotonation of **A** to form enolate **A''** is predicted to be exergonic by 8.4 kcal/mol.[30] This

deprotonation process is in part entropy-driven as the enolate oxygen replaces the acetate ligand in **A** to form a six-membered chelation with the Pd center.

Scheme 3. Kinetics Experiments

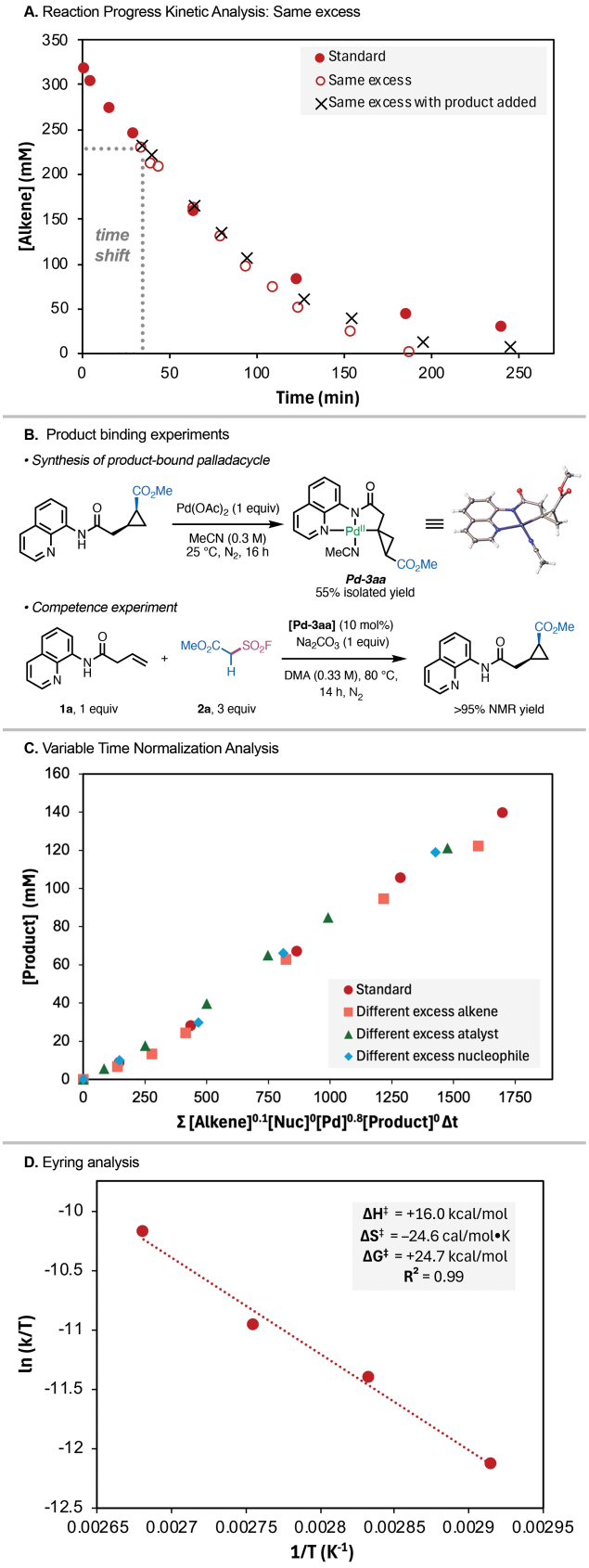

Due to the ablation of the new α-stereocenter formed after nucleopalladation, under the Curtin–Hammett conditions, the product diastereoselectivity is determined in the subsequent steps. Our calculations indicate that the oxidative addition proceeds via an S_N2-type stereoinvertive mechanism (**TS2** and **TS2'**). Other oxidative addition pathways, including the four- and three-centered C–S oxidative addition (**TS4–TS6**, Scheme 4B) and the S–F oxidative addition[13,14] (Figure S6) were found to be less favorable. Subsequent reductive elimination from the Pd^{IV} intermediate **B** (**TS3**) is kinetically facile with a low barrier of 1.7 kcal/mol with respect to **B**, consistent with our recent computational study on the strain-release-promoted reductive elimination from Pd^{IV} to form cyclopropane rings.[17] The computed reaction energy profile indicates that the irreversible intramolecular S_N2-type oxidative addition (**TS2**) is the rate- and diastereoselectivity-determining step. The computed overall barrier from the Pd–enolate resting state **A''** to **TS2** ($\Delta G^{\ddagger}$ = 28.7 kcal/mol, $\Delta H^{\ddagger}$ = 17.5 kcal/mol) is in good agreement with the experimentally determined activation parameters. The large negative activation entropy ($\Delta S^{\ddagger}$ = −31.7 e.u. compared with the experimental value of −24.6 e.u.) is primarily attributed to entropy loss during the association of an OAc^- ligand upon reprotonation of the enolate resting state **A''**. The computed diastereoselectivity indicates that the S_N2-type oxidative addition via **TS2** leading to the *cis*-cyclopropane product is 3.0 kcal/mol more favorable than the minor pathway via **TS2'** leading to the *trans* product, which is consistent with the experimentally observed diastereoselectivity (>20:1 *d.r.*). **TS2'** is destabilized by steric interactions between the acetate ligand and the ester group.

In conclusion, a highly diastereoselective Pd^{II}/Pd^{IV} catalyzed cyclopropanation of unactivated alkenes with alkyl sulfonyl fluorides has been developed. The synthetic versatility of this method stems from the diverse array of pronucleophiles that are compatible. With internal alkenes, all *cis*-substituted cyclopropanes that are otherwise difficult to access can be prepared in one step. Kinetic experiments and DFT calculations indicate that the S_N2-type oxidative addition is the rate- and diastereoselectivity-determining step.

Scheme 4. (A) DFT-computed reaction energy profile of the formation of cyclopropane 3aa; (B) Oxidative addition transition states. All Gibbs free energies and enthalpies are with respect to Pd-1.

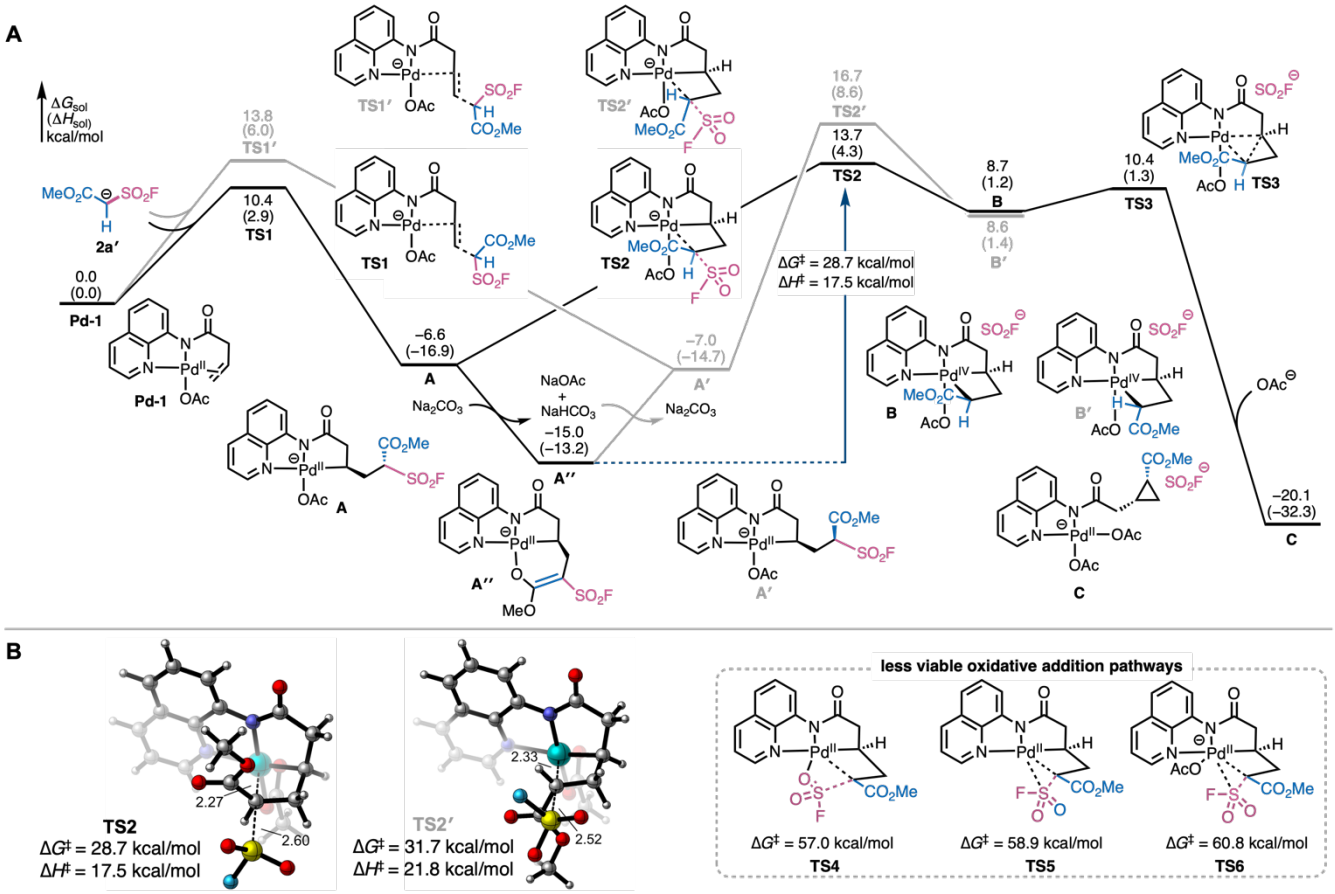

ASSOCIATED CONTENT

Supporting Information. This material is available free of charge via the Internet at http://pubs.acs.org."
Experimental procedures, compound characterization, computational details, Cartesian coordinates of computed structures, X-ray crystallography, and NMR spectra (PDF) NMR data (MNova format) (ZIP)

Accession Codes CCDC 2171740 (**(±)-3aa**), CCDC 2345363 (**(±)-3aj**), CCDC 2351469 (**(±)-3al'**), CCDC 2345089 (**(±)-4aa**), CCDC 2376390 (**(±)-4ad**), CCDC 2367118 (**(±)-4ah**), CCDC 2394329(**(±)-6aa**), and CCDC 2171739 (**Pd-3aa**) contain the supplementary crystallographic data for this paper. These data can be obtained free of charge via www.ccdc.cam.ac.uk/data_request/cif, or by emailing data_request@ccdc.cam.ac.uk, or by contacting The Cambridge Crystallographic Data Centre, 12 Union Road, Cambridge CB2 1EZ, UK; fax: +44 1223 336033.

AUTHOR INFORMATION

Corresponding Author

Peng Liu –Department of Chemistry, University of Pittsburgh, 219 Parkman Avenue, Pittsburgh, Pennsylvania 15260, United States; orcid.org/0000-0002-8188-632X; Email: pengliu@pitt.edu

K. Barry Sharpless – Department of Chemistry, The Scripps Research Institute, La Jolla, California 92037, United States; orcid.org/0000-0001-6051-1599; Email: sharples@scripps.edu

Keary M. Engle – Department of Chemistry, The Scripps Research Institute, La Jolla, California 92037, United States; orcid.org/0000-0003-2767-6556; Email: keary@scripps.edu

Authors

Yilin Cao – Department of Chemistry, The Scripps Research Institute, 10550 North Torrey Pines Road, La Jolla, California 92037, United States; orcid.org/0000-0002-4964-0565

Warabhorn Rodphon – Department of Chemistry, The Scripps Research Institute, 10550 North Torrey Pines Road, La Jolla, California 92037, United States

Turki M. Alturaifi – Department of Chemistry, University of Pittsburgh, 219 Parkman Avenue, Pittsburgh, Pennsylvania 15260, United States; orcid.org/0000-0002-6379-1669

Al Vicente Riano D. Lisboa – Department of Chemistry, The Scripps Research Institute, 10550 North Torrey Pines Road, La

Jolla, California 92037, United States; orcid.org/0009-0008-4902-2522

Zhouyang Ren – Department of Chemistry, The Scripps Research Institute, 10550 North Torrey Pines Road, La Jolla, California 92037, United States; orcid.org/0009-0002-5335-1034

Job J. C. Struijs – Department of Chemistry, The Scripps Research Institute, 10550 North Torrey Pines Road, La Jolla, California 92037, United States; orcid.org/0000-0002-6051-2927

Hui-Qi Ni – Department of Chemistry, The Scripps Research Institute, 10550 North Torrey Pines Road, La Jolla, California 92037, United States; orcid.org/0009-0006-4848-638X

Taras Savchuk – Enamine Ltd., Chervonotkatska 78, 02094 Kyiv, Ukraine; Kukhar Institute of Bioorganic Chemistry and Petrochemistry NAS of Ukraine, 02094 Kyiv, Ukraine.

Pavel K. Mykhailiuk – Enamine Ltd., Chervonotkatska 78, 02094 Kyiv, Ukraine; Taras Shevchenko National University of Kyiv, Faculty of Chemistry, Volodymyrska 60, 01601 Kyiv, Ukraine; orcid.org/0000-0003-1821-9011

Richard P. Loach – Pfizer Medicinal Sciences, Eastern Point Road, Groton, Connecticut 06340, United States

Shouliang Yang – Pfizer Oncology Medicinal Chemistry 10770 Science Center Drive, San Diego, CA 92121, United States

Indrawan J. McAlpine – Pfizer Oncology Medicinal Chemistry 10770 Science Center Drive, San Diego, CA 92121, United States; Genesis Therapeutics, 11568 Sorrento Valley Rd. Suite 8, San Diego, California 92121, United States; orcid.org/0000-0002-4230-4892

Donna G. Blackmond – Department of Chemistry, The Scripps Research Institute, La Jolla, California 92037, United States; orcid.org/ 0000-0001-9829-8375

Notes

The authors declare no competing financial interest.

ACKNOWLEDGMENT

This work was financially supported by the U.S. National Science Foundation (CHE-2046286, KME), the U.S. National Institutes of Health (R35 GM128779), Pfizer, Inc., and Enamine Ltd. We thank the David C. Fairchild Endowed Fellowship Fund for a Graduate Fellowship (Y.C.), the National Research Council of Thailand (NRCT5-RGJ63023-177) for a predoctoral fellowship (W.R.), the Skaggs Endowed Fellowship program for a Graduate Fellowship (Z.R.), the Schimmel Family Endowed Fellowship Fund for a Graduate Fellowship (A.V.R.D.L.), and the EPSRC for studentship (EP/S023828/1) funding through the OxICFM CDT (J.J.C.S). We further thank Dr. Jake Bailey (UCSD) Dr. Milan Gembicky (UCSD), Shenghua Yang (Scripps Research), and Dr. S. Shishkina (IOC, Kyiv) for X-ray crystallographic analysis. We are grateful to Dr. Jason S. Chen, Brittany B. Sanchez, Quynh Nguyen Wong, and Jason Lee (Scripps Research Automated Synthesis Facility) for assistance with SFC and HRMS analysis. DFT calculations were carried out at the University of Pittsburgh Center for Research Computing and the Advanced Cyberinfrastructure Coordination Ecosystem: Services & Support (ACCESS) program, supported by NSF award numbers OAC-2117681, OAC-1928147. and OAC-1928224. We also thank Jinhan Yu (Scripps Research), Dr. Min Deng (Scripps Research), and Dr. Ester Maria Di Tommaso (Scripps Research) for helpful discussion.

REFERENCES

(1) (a) Chinthakindi, P. K.; Arvidsson, P. I. Sulfonyl Fluorides (SFs): More than Click Reagents? *Eur. J. Org. Chem* **2018**, 3648–3666. (b) Zhao, C.; Rakesh, K. P.; Ravidar, L.; Fang, W.-Y.; Qin, H.-L. Pharmaceutical and Medicinal Significance of Sulfur (S^{VI})-Containing Motifs for Drug Discovery: A Critical Review. *Eur. J. Med. Chem*. **2019**, *162*, 679–734.

(2) Lou, T. S.-B.; Willis, M. C. Sulfonyl Fluorides as Targets and Substrates in the Development of New Synthetic Methods. *Nat. Rev. Chem.* **2022**, *6*, 146–162.

(3) Narayanan, A.; Jones, L. H. Sulfonyl Fluorides as Privileged Warheads in Chemical Biology. *Chem. Sci.* **2015**, *6*, 2650–2659.

(4) Dong, J.; Krasnova, L.; Finn, M. G.; Sharpless, K. B. Sulfur(VI) Fluoride Exchange (SuFEx): Another Good Reaction for Click Chemistry. *Angew. Chem. Int. Ed.* **2014**, *53*, 9430–9448.

(5) Barrow, A. S.; Smedley, C. J.; Zheng, Q.; Li, S.; Dong, J.; Moses, J. E. The Growing Applications of SuFEx Click Chemistry. *Chem. Soc. Rev.* **2019**, *48*, 4731–4758.

(6) Representative papers on the synthesis organosulfonyl fluorides: (a) Tribby, A. L.; Rodríguez, I.; Shariffudin, S.; Ball, N. D. Pd-Catalyzed Conversion of Aryl Iodides to Sulfonyl Fluorides Using SO_2 Surrogate DABSO and Selectfluor. *J. Org. Chem.* **2017**, *82*, 2294–2299. (b) Kwon, J.; Kim, B. M. Synthesis of Arenesulfonyl Fluorides via Sulfuryl Fluoride Incorporation from Arynes. *Org. Lett.* **2019**, *21*, 428–433. (c) Laudadio, G.; Bartolomeu, A. d. A.; Verwijlen, L. M. H. M.; Cao, Y.; de Oliveira, K. T.; Noël, T. Sulfonyl Fluoride Synthesis through Electrochemical Oxidative Coupling of Thiols and Potassium Fluoride. *J. Am. Chem. Soc.* **2019**, *141*, 11832–11836. (d) Lee, C.; Ball, N. D.; Sammis, G. M. One-Pot Fluorosulfurylation of Grignard Reagents Using Sulfuryl Fluoride. *Chem. Commun*. **2019**, *55*, 14753–14756. (e) Smedley, C. J.; Li, G.; Barrow, A. S.; Gialelis, T. L.; Giel, M.-C.; Ottonello, A.; Cheng, Y.; Kitamura, S.; Wolan, D. W.; Sharpless, K. B.; Moses, J. E. Diversity Oriented Clicking (DOC): Divergent Synthesis of SuFExable Pharmacophores from 2-Substituted-Alkynyl-1-Sulfonyl Fluoride (SASF) Hubs. *Angew. Chem. Int. Ed.* **2020**, *59*, 12460–12469. (f) Erchinger, J. E.; Hoogesteger, R.; Laskar, R.; Dutta, S.; Hümpel, C.; Rana, D.; Daniliuc, C. G.; Glorius, F. EnT-Mediated N–S Bond Homolysis of a Bifunctional Reagent Leading to Aliphatic Sulfonyl Fluorides. *J. Am. Chem. Soc.* **2023**, *145*, 2364–2374.

(7) Chinthakindi, P. K.; Kruger , H. G.; Govender, T.; Naicker, T.; Arvidsson,P. I. On-Water Synthesis of Biaryl Sulfonyl Fluorides. *J. Org. Chem.* **2016**, *81*, 2618–2623.

(8) Cherepakha, A. Y.; Stepannikova, K. O.; Vashchenko, B. V.; Gorichko, M. V.; Tolmachev, A. A.; Grygorenko, O. O. Hetaryl Bromides Bearing the SO_2F Group – Versatile Substrates for Palladium-Catalyzed C–C Coupling Reactions. *Eur. J. Org. Chem.* **2018,** 6682–6692.

(9) (a) Lou, T. S.-B.; Willis, M. C. Arylsulfonyl Fluoride Boronic Acids: Preparation and Coupling Reactivity. *Tetrahedron* **2020,** *76*, 130782. (b) Nielsen, M. K.; Ugaz, C. R.; Li, W.; Doyle, A. G. PyFluor: A Low-Cost, Stable, and Selective Deoxyfluorination Reagent. *J. Am. Chem. Soc.* **2015**, *137*, 9571–9574.

(10) Chen, Q.; Mayer, P.; Mayr, H. Ethenesulfonyl Fluoride: The Most Perfect Michael Acceptor Ever Found? *Angew. Chem. Int. Ed.* **2016**, *55*, 12664–12667.

(11) Qin, H.-L.; Zheng, Q.; Bare, G. A. L.; Wu, P.; Sharpless, K. B. A Heck–Matsuda Process for the Synthesis of β-Arylethenesulfonyl Fluorides: Selectively Addressable Bis-Electrophiles for SuFEx Click Chemistry. *Angew. Chem. Int. Ed.* **2016**, *55*, 14155–14158.

(12) Zha, G.-F.; Zheng, Q.; Leng, J.; Wu, P.; Qin, H.-L.; Sharpless, K. B. Palladium-Catalyzed Fluorosulfonylvinylation of Organic Iodides. *Angew. Chem. Int. Ed.* **2017**, *56*, 4849–4852.
(13) Chatelain, P.; Muller, C.; Sau, A.; Brykczyńska, D.; Bahadori, M.; Rowley, C. N.; Moran, J. Desulfonative Suzuki–Miyaura Coupling of Sulfonyl Fluorides. *Angew. Chem. Int. Ed.* **2021**, *60*, 25307–25312.
(14) Zhang, G.; Guan, C.; Zhao, Y.; Miao, H.; Ding, C. "Awaken" Aryl Sulfonyl Fluoride: A New Partner in the Suzuki–Miyaura Coupling Reaction. *New. J. Chem.* **2022**, *46*, 3560–3564.
(15) (a)Hawkins, J. M.; Lewis, T. A.; Raw, A. S. Substituent Effects on Sulfonate Ester Based Olefinations. *Tetrahedron Lett.* **1990**, *31*, 981–984. (b) Kagabu, S.; Hara, K.; Takahashi, J. Alkene Formation through Condensation of Phenylmethanesulphonyl Fluoride with Carbonyl Compounds. *J. Chem. Soc., Chem. Commun.* **1991**, 408–410. (c) Kagabu S.; Shimizu C.; Takahashi J.; Hara K.; Koketsu M.; Ishida M. Reaction of Phenyl- and Alkoxycarbonylmethanesulfonyl Fluoride with Activated Haloalkanes. *Bull. Soc. Chim. Fr.* **1992**, *129*, 435–439. (d) Górski, B.; Talko, A.; Basak, T.; Barbasiewicz, M. Olefination with Sulfonyl Halides and Esters: Scope, Limitations, and Mechanistic Studies of the Hawkins Reaction. *Org. Lett.* **2017**, *19*, 1756–1759. (e) Górski, B.; Basiak, D.; Talko, A.; Basak, T.; Mazurek, T.; Barbasiewicz, M. Olefination with Sulfonyl Halides and Esters: E-Selective Synthesis of Alkenes from Semistabilized Carbanion Precursors. *Eur. J. Org. Chem.* **2018**, 1774–1784. (f) Tryniszewski, M.; Basiak, D.; Barbasiewicz, M. Olefination with Sulfonyl Halides and Esters: Synthesis of Unsaturated Sulfonyl Fluorides. *Org. Lett.* **2022**, *24*, 4270–4274.
(16) Liang, H.; Liu, Q.; Zhao, X.; He, T.; Luo, J.; Huang, S. Amidation of β-Keto Sulfonyl Fluorides via C–C Bond Cleavage. *Eur. J. Org. Chem.* **2024**, e202400391.
(17) Ni, H.-Q.; Alturaifi, T. M.; Rodphon, W.; Scherschel, N. F.; Yang, S.; Wang, F.; McAlpine, I. J.; Piercey, D. G.; Liu, P.; Engle, K. M. *Anti*-selective Cyclopropanation of Nonconjugated Alkenes with Diverse Pronucleophiles via Directed Nucleopalladation. *J. Am. Chem. Soc.* **2024**, *146*, 24503–24514.
(18) For reviews, see: (a) Davies, H. M. L.; Antoulinakis, E. Intermolecular Metal-Catalyzed Carbenoid Cyclopropanations. *Org. React.* **2001**, *57*, 1–326. (b) Lebel, H.; Marcoux, J.-F.; Molinaro, C.; Charette, A. B. Stereoselective Cyclopropanation Reactions. *Chem. Rev.* **2003**, *103*, 977–1050. (c) Maas, G. Ruthenium-Catalysed Carbenoid Cyclopropanation Reactions with Diazo Compounds. *Chem. Soc. Rev.* **2004**, *33*, 183–190. (d) Ford, A.; Miel, H.; Ring, A.; Slattery, C. N.; Maguire, A. R.; McKervey, M. A. Modern Organic Synthesis with α-Diazocarbonyl Compounds. *Chem. Rev.* **2015**, *115*, 9981–10080.
(19) Representative reports on synthesis of *cis*-cyclopropanes: (a) Lévesque, É.; Goudreau, S. R.; Charette, A. B. Improved Zinc-Catalyzed Simmons–Smith Reaction: Access to Various 1,2,3-Trisubstituted Cyclopropanes. *Org. Lett.* **2014**, *16*, 1490–1493. (b) Yasui, M.; Ota, R.; Tsukano, C.; Takemoto, Y. Synthesis of *cis*-/All-*cis*-Substituted Cyclopropanes through Stereocontrolled Metalation and Pd-Catalyzed Negishi Coupling. *Org. Lett.* **2018**, *20*, 7656–7660. (c) Piou, T.; Romanov-Michailidis, F.; Ashley, M. A.; Romanova-Michaelides, M.; Rovis, T. Stereodivergent Rhodium(III)-Catalyzed *cis*-Cyclopropanation Enabled by Multivariate Optimization. *J. Am. Chem. Soc.* **2018**, *140*, 9587–9593. (d) Phipps, E. J. T.; Rovis, T. Rh(III)-Catalyzed C–H Activation-Initiated Directed Cyclopropanation of Allylic Alcohols. *J. Am. Chem. Soc.* **2019**, *141*, 6807–6811. (e) Costantini, M.; Mendoza, A. Modular Enantioselective Synthesis of *Cis*-Cyclopropanes through Self-Sensitized Stereoselective Photodecarboxylation with Benzothiazolines. *ACS Catal.* **2021**, *11*, 13312–13319. (f) Mato, M.; Herlé, B.; Echavarren, A. M. Cyclopropanation by Gold- or Zinc-Catalyzed Retro-Buchner Reaction at Room Temperature. *Org. Lett.* **2018**, *20*, 4341–4345.
(20) James, G. T. Inactivation of the Protease Inhibitor Phenylmethylsulfonyl Fluoride in Buffers. *Anal. Biochem.* **1978**, *86*, 574–579.
(21) Antermite, D.; Affron, D. P.; Bull, J. A. Regio- and Stereoselective Palladium-Catalyzed C(sp^3)–H Arylation of Pyrrolidines and Piperidines with C(3) Directing Groups. *Org. Lett.* **2018**, *20*, 3948–3952.
(22) Blackmond, D. G. Reaction Progress Kinetic Analysis: A Powerful Methodology for Mechanistic Studies of Complex Catalytic Reactions. *Angew. Chem. Int. Ed.* **2005**, *44*, 4302–4320.
(23) Hoshiya, N.; Kobayashi, T.; Arisawa, M.; Shuto, S. Palladium-Catalyzed Arylation of Cyclopropanes via Directing Group-Mediated C(sp^3)–H Bond Activation to Construct Quaternary Carbon Centers: Synthesis of *cis*- and *trans*-1,1,2-Trisubstituted Chiral Cyclopropanes. *Org. Lett.* **2013**, *15*, 6202–6205.
(24) Nielsen, C. D.-T.; Burés, J. Visual Kinetic Analysis. *Chem. Sci.* **2019**, *10*, 348–353.
(25) Anslyn, E. V.; Dougherty, D. A. *Modern Physical Organic Chemistry;* University Science Books: Sausalito, California, 2008.
(26) The DFT calculations were performed at the ωB97X-D/def2-TZVP/SMD(DMA)//B3LYP-D3(BJ)/6-31G(d)–SDD(Pd) level of theory. The reaction energy profile was calculated at the experimental reaction temperature (80 °C). See the Supporting Information for computational details.
(27) The deprotonation of **2a** to form **2a'** is expected to be facile based on its predicted pK_a value of 6.83 and the experimental pK_a of 7.75 for the analogous trifluoromethanesulfonyl in water (see Figure S10 for details).
(28) For experimental pK_a of $EtO_2C–CH_2–SO_2CF_3$ see: Goumont, R.; Magnier, E.; Kizilian, E.; Terrier, F. Acidity Inversions of α-NO_2 and α-SO_2CF_3 Activated Carbon Acids as a Result of Contrasting Solvent Effects on Transfer from Water to Dimethyl Sulfoxide Solutions. *J. Org. Chem.* **2003**, *68*, 6566–6570.
(29) The predicted pK_a value was obtained using Rowan's pK_a prediction workflow that utilizes the second-generation atoms-in-molecules neural network potential (AIMNet2). See: (a) Wagen, C. C.; Wagen, A. M. Efficient and Accurate pK_a Prediction Enabled by Pre-Trained Machine-Learned Interatomic Potentials. *ChemRxiv* **2024**, DOI: 10.26434/chemrxiv-2024-8489b. (b) Anstine, D. M.; Zubatyuk, R.; Isayev, O. AIMNet2: A Neural Network Potential to Meet Your Neutral, Charged, Organic, and Elemental-Organic Needs. *ChemRxiv* **2024**, DOI: 10.26434/chemrxiv-2023-296ch-v2
(30) Two explicit DMA solvent molecules were used in the calculations to coordinate to each Na atom in Na_2CO_3, $NaHCO_3$, and NaOAc. See Figure S5 for details.